Theoretical analysis of radiation-induced magnetoresistance oscillations in high-mobility two-dimensional electron systems

2004 J. Phys.: Condens. Matter 16 4045

(http://iopscience.iop.org/0953-8984/16/23/021)

INSTITUTE OF PHYSICS PUBLISHING JOURNAL OF PHYSICS: CONDENSED MATTER

J. Phys.: Condens. Matter **16** (2004) 4045–4060 PII: S0953-8984(04)75761-6

Theoretical analysis of radiation-induced magnetoresistance oscillations in high-mobility two-dimensional electron systems

X L Lei

Department of Physics, Shanghai Jiaotong University, 1954 Huashan Road, Shanghai 200030, People's Republic of China

Received 3 February 2004
Published 28 May 2004
Online at stacks.iop.org/JPhysCM/16/4045
DOI: 10.1088/0953-8984/16/23/021

Abstract

We present a detailed theoretical investigation of the radiation induced giant magnetoresistance oscillations recently discovered in high-mobility two-dimensional electron gas. Electron interactions with impurities, and transverse and longitudinal acoustic phonons in GaAs-based heterosystems are considered simultaneously. Multiphoton-assisted impurity scatterings are shown to be the primary origin of the resistance oscillation. Based on the balance-equation theory developed for magnetotransport in Faraday geometry, we are able not only to reproduce the observed period, phase and the negative resistivity of the main oscillations, but also to predict the secondary peak/valley structures relating to two-photon and three-photon processes. The dependence of the magnetoresistance oscillation on microwave intensity, the role of dc bias current and the effect of elevated electron temperature are discussed. Furthermore, we propose that the temperature dependence of the resistance oscillation stems from the growth of the Landau level broadening due to the enhancement of acoustic phonon scattering with increasing lattice temperature. The calculated temperature variation of the oscillation agrees well with experimental observations.

1. Introduction

Tremendous interest in magneto-transport in two-dimensional electron systems (2DESs) has recently been revived since the experimental discovery of giant oscillations of the longitudinal resistance as a function of the magnetic field in high mobility two-dimensional (2D) electron gas (EG) subjected to microwave radiation [1–3], particularly following the recent observations of 'zero-resistance' states in very clean samples by two independent groups [4–7]. These radiation-induced oscillations of the longitudinal magnetoresistivity R_{xx} are periodical in inverse magnetic field $1/B$ with the period determined by the radiation frequency ω rather

than by the electron density N_e [8]. The observed R_{xx} oscillations exhibit a smooth magnetic-field variation with the resistivity maxima at $\omega/\omega_c = j - \delta_-$ and minima at $\omega/\omega_c = j + \delta_+$ (ω_c is the cyclotron frequency, $j = 1, 2, 3, \ldots$) having positive $\delta_\pm$ ranging around 0.1–0.25 [4, 7]. The resistivity minimum goes downward with increasing sample mobility and/or increasing radiation intensity until a vanishing resistance state shows up, while the Hall resistivity keeps the classical form $R_{xy} = B/eN_e$ with no sign of quantum Hall plateau over the whole magnetic field range exhibiting R_{xx} oscillation. Later independent experiments [9, 10] confirmed these results and the corresponding zero-conductance states were also observed in the Corbino samples [11].

To explore the origin of these peculiar 'zero-resistance' states, different mechanisms have been suggested [12–19]. As is shown by Andreev *et al* [13], a negative linear conductance implies that the zero current state is intrinsically unstable: the system spontaneously develops a non-vanishing local current density which is determined by the condition that the component of the electric field parallel to the local current vanishes. Thus the appearance of negative longitudinal resistivity or conductivity in a uniform model suffices to explain the observed vanishing resistance. The possibility of absolute negative photoconductance in a 2DES subject to a perpendicular magnetic field was first explored 30 years ago by Ryzhii [20, 21]. Experimentally Keay *et al* [22] reported the observation of absolute negative conductance in sequential resonant tunnelling superlattices driven by intense terahertz radiation. Recent works [12, 14, 15] indicated that the periodical structure of the density of states (DOS) of the 2DEG in a magnetic field and the photon-excited electron scatterings by impurities are the main origin of the magnetoresistance oscillations. Durst *et al* [12] proposed a microscopic analysis for the conductivity assuming a δ-correlated disorder and a simple form of the 2D electron self-energy oscillatory with the magnetic field, obtaining the correct period, phase and the possible negative resistivity. Shi and Xie [15] gave a similar result using the Tien and Gorden current formula [23] for photon-assisted coherent tunnelling. A more quantitative theoretical description was reported recently using a balance equation approach developed for radiation-induced magnetotransport in Faraday geometry [24], not only reproducing the correct period, phase and the negative resistivity of the main oscillations, but also predicting the secondary peaks and additional maxima and minima observed in the experiment [5, 7, 9], and identifying them as arising from double- and triple-photon processes. A quantum Boltzmann equation approach based on a self-consistent Born approximation for large filling factors has also been presented very recently, taking account of the elastic (impurity) scattering as the major mechanism for radiation-induced magnetoresistance oscillation [25]. In addition to the photon-assisted impurity scattering referred to above as the mechanism of the absolute negative conductivity (ANC), other possible mechanisms were also explored in the literature. Ryzhii *et al* proposed that acoustic phonon scattering [26, 27] and heating of electrons [28] could also serve as the mechanisms of ANC in 2DESs, and made a further attempt to connect them with experiments [29].

One of the most important and interesting features of this phenomenon is its sensitive temperature dependence. The 'zero-resistance' states and radiation-induced magnetoresistance oscillations show up strongly only at low temperatures typically around $T = 1$ K or lower. At fixed microwave power with increasing temperature, not only the zero-resistance regions become narrower and eventually disappear, the whole oscillatory structure (peaks and valleys) diminish as well. At temperature $T \geqslant 4$–5 K, the oscillatory structure disappears completely and the resistivity R_{xx} versus magnetic field becomes essentially structureless [4, 5]. The temperature variation of the resistivity at deepest minima exhibits approximate activated-type behaviour $R_{xx} \propto \exp(-T_0/T)$. However, the activation energies T_0 observed by both groups are very high: up to 10 and 20 K at $j = 1$ minimum [4, 5]. These

values are much higher than the microwave photon energy ($\omega \sim 3$–5 K) and Landau-level spacing ($\omega_c \leqslant \omega$). Furthermore, different T_0 values observed by the two groups indicate that the disappearing speed of the oscillatory structure with increasing temperature is sample dependent [4, 5]. To my knowledge, there has been no theoretical attempt to explain this temperature dependence, except that a conjecture of the formation of an energy gap around the Fermi surface is suggested under microwave irradiation around the resistance minima [4].

The recently constructed balance-equation model [24, 30], which provides a quantitative and tractable approach to radiation-induced magnetotransport in Faraday geometry, enables us not only to analyse the magnetoresistance oscillation, its dependence on the radiation intensity, but also to deal with its temperature variation in a comprehensive way. We suggest that the temperature suppression of the magnetoresistance oscillation in these high-mobility 2DESs comes mainly from the growth of the Landau level broadening due to the rapid enhancement of acoustic phonon scatterings with increasing temperature in this low temperature range.

In this paper we will carry out a detailed theoretical investigation on the different aspects of radiation-induced magnetoresistance oscillation. The paper is organized as follows. For convenience and completeness we present the general theoretical model and formulation in section 2. As a typical example we analyse GaAs-based systems for which the relevant material parameters are discussed in section 3. Section 4 concentrates on the transport properties of GaAs-based heterosystems at lattice temperature $T = 1$ K. We will give a detailed discussion on the impurity and acoustic phonon scattering related linear and nonlinear magnetoresistance induced by the irradiation of 0.1 THz microwaves of different intensities, and the effect of elevated electron temperature. Section 5 is devoted to the analysis of the lattice-temperature dependence of the magnetoresistance oscillation. Finally, a brief summary is given in section 6.

2. Formulation

2.1. Balance equations in crossed electric and magnetic fields

The experiments allow us to assume the 2DEG being in extended states over the magnetic field range relevant to this phenomenon. For a general treatment, we consider N_e electrons in a unit area of a quasi-2D system in the x–y plane with a confining potential $V(z)$ in the z-direction. These electrons, besides interacting with each other, are scattered by random impurities/disorders and by phonons in the lattice. To include possible elliptically polarized microwave illumination we assume that a uniform dc electric field $\mathbf{E}_0$ and a high-frequency (HF) ac field of frequency ω,

$$\mathbf{E}_t \equiv \mathbf{E}_s \sin(\omega t) + \mathbf{E}_c \cos(\omega t), \tag{1}$$

are applied in the x–y plane, together with a magnetic field $\mathbf{B} = (0, 0, B)$ along the z direction. In terms of the 2D centre-of-mass momentum and coordinate of the electron system [33, 31, 32], which are defined as $\mathbf{P} \equiv \sum_j \mathbf{p}_{j\|}$ and $\mathbf{R} \equiv N_e^{-1} \sum_j \mathbf{r}_{j\|}$, with $\mathbf{p}_{j\|} \equiv (p_{jx}, p_{jy})$ and $\mathbf{r}_{j\|} \equiv (x_j, y_j)$ being the momentum and coordinate of the jth electron in the 2D plane, and the relative electron momentum and coordinate $\mathbf{p}'_{j\|} \equiv \mathbf{p}_{j\|} - \mathbf{P}/N_e$ and $\mathbf{r}'_{j\|} \equiv \mathbf{r}_{j\|} - \mathbf{R}$, the Hamiltonian of the system can be written as the sum of a centre-of-mass part H_{cm} and a relative electron part H_{er} ($\mathbf{A}(\mathbf{r})$ is the vector potential of the $\mathbf{B}$ field),

$$H_{cm} = \frac{1}{2N_e m}(\mathbf{P} - N_e e\mathbf{A}(\mathbf{R}))^2 - N_e e(\mathbf{E}_0 + \mathbf{E}_t) \cdot \mathbf{R}, \tag{2}$$

$$H_{er} = \sum_j \left[\frac{1}{2m} \left(\mathbf{p}'_{j\|} - e\mathbf{A}(\mathbf{r}'_{j\|}) \right)^2 + \frac{p_{jz}^2}{2m_z} + V(z_j) \right] + \sum_{i<j} V_c(\mathbf{r}'_{i\|} - \mathbf{r}'_{j\|}, z_i, z_j), \tag{3}$$

together with electron–impurity and electron–phonon interactions $H_{\rm ei}$ and $H_{\rm ep}$. Here m and m_z are, respectively, the electron effective mass parallel and perpendicular to the plane, and $V_{\rm c}$ stands for the electron–electron Coulomb interaction. It should be noted that the uniform electric field (dc and ac) appears only in $H_{\rm cm}$, and that $H_{\rm er}$ is just the Hamiltonian of a quasi-2D system subjected to a magnetic field. The coupling between the centre-of-mass and the relative electrons exists via the electron–impurity and electron–phonon interactions. Our treatment starts with the Heisenberg operator equations for the rates of changes of the centre-of-mass velocity $\dot{\mathbf{V}} = -{\rm i}[\mathbf{V}, H] + \partial\mathbf{V}/\partial t$, with $\mathbf{V} = -{\rm i}[\mathbf{R}, H]$, and of the relative electron energy $\dot{H}_{\rm er} = -{\rm i}[H_{\rm er}, H]$, and proceeds with the determination of their statistical averages.

As proposed in [31], the centre-of-mass coordinate $\mathbf{R}$ and velocity $\mathbf{V}$ can be treated classically, i.e. as the time-dependent expectation values of the centre-of-mass coordinate and velocity, $\mathbf{R}(t)$ and $\mathbf{V}(t)$, such that $\mathbf{R}(t)-\mathbf{R}(t') = \int_{t'}^{t} \mathbf{V}(s)\,{\rm d}s$. We are concerned with the steady transport state under an irradiation of single frequency and focus on the photon-induced dc resistivity and the energy absorption of the HF field. These quantities are directly related to the time-averaged and/or base-frequency oscillating components of the centre-of-mass velocity. Although higher harmonics of the current may affect the dc and lower harmonic terms of the drift velocity through entering the damping force and energy exchange rates in the resulting equations, in an ordinary semiconductor the power of even the third harmonic current is rather weak as compared to the fundamental. For the HF field intensity in the experiments, the effect of higher harmonic current is safely negligible. Hence, it suffices to assume that the centre-of-mass velocity, i.e. the electron drift velocity, consists of a dc part $\mathbf{v}_0$ and a stationary time-dependent part $\mathbf{v}(t)$ of the form

$$\mathbf{V}(t) = \mathbf{v}_0 + \mathbf{v}_1\cos(\omega t) + \mathbf{v}_2\sin(\omega t). \tag{4}$$

With this, the exponential factor in the operator equations can be expanded in terms of Bessel functions $J_n(x)$:

$$\mathrm{e}^{-{\rm i}\mathbf{q}\cdot\int_{t'}^{t}\mathbf{V}(s)\,{\rm d}s} = \sum_{n=-\infty}^{\infty} J_n^2(\xi)\mathrm{e}^{{\rm i}(\mathbf{q}\cdot\mathbf{v}_0-n\omega)(t-t')} + \sum_{m\neq 0}\mathrm{e}^{{\rm i}m(\omega t-\varphi)}\sum_{n=-\infty}^{\infty} J_n(\xi)J_{n-m}(\xi)\mathrm{e}^{{\rm i}(\mathbf{q}\cdot\mathbf{v}_0-n\omega)(t-t')}.$$

Here the argument in the Bessel functions

$$\xi \equiv \frac{1}{\omega}\left[(\mathbf{q}_\parallel\cdot\mathbf{v}_1)^2 + (\mathbf{q}_\parallel\cdot\mathbf{v}_2)^2\right]^{\frac{1}{2}} \tag{5}$$

and $\tan\varphi = (\mathbf{q}\cdot\mathbf{v}_2)/(\mathbf{q}\cdot\mathbf{v}_1)$. On the other hand, for 2D systems having electron sheet density of the order of 10^{15} m^{-2}, the intra-band and inter-band Coulomb interactions are sufficiently strong that it is adequate to describe the relative-electron transport state using a single electron temperature $T_{\rm e}$. Apart from this, the electron–electron interaction is treated only in a mean-field level under random phase approximation (RPA) [31, 32]. For the determination of the unknown parameters $\mathbf{v}_0$, $\mathbf{v}_1$, $\mathbf{v}_2$ and $T_{\rm e}$, it suffices to know the damping force up to the base frequency oscillating term $\mathbf{F}(t) = \mathbf{F}_0 + \mathbf{F}_{\rm s}\sin(\omega t) + \mathbf{F}_{\rm c}\cos(\omega t)$, and the energy-related quantities up to the time-average term. We finally obtain the force and energy balance equations:

$$0 = N_{\rm e}e\mathbf{E}_0 + N_{\rm e}e(\mathbf{v}_0\times\mathbf{B}) + \mathbf{F}_0, \tag{6}$$

$$\mathbf{v}_1 = \frac{e\mathbf{E}_{\rm s}}{m\omega} + \frac{\mathbf{F}_{\rm s}}{N_{\rm e}m\omega} - \frac{e}{m\omega}(\mathbf{v}_2\times\mathbf{B}), \tag{7}$$

$$-\mathbf{v}_2 = \frac{e\mathbf{E}_{\rm c}}{m\omega} + \frac{\mathbf{F}_{\rm c}}{N_{\rm e}m\omega} - \frac{e}{m\omega}(\mathbf{v}_1\times\mathbf{B}), \tag{8}$$

$$N_{\rm e}e\mathbf{E}_0\cdot\mathbf{v}_0 + S_{\rm p} - W = 0. \tag{9}$$

Here

$$\mathbf{F}_0 = \sum_{\mathbf{q}_\parallel} \left|U(\mathbf{q}_\parallel)\right|^2 \sum_{n=-\infty}^{\infty} \mathbf{q}_\parallel J_n^2(\xi)\Pi_2(\mathbf{q}_\parallel, \omega_0 - n\omega) + \sum_{\mathbf{q}} |M(\mathbf{q})|^2 \sum_{n=-\infty}^{\infty} \mathbf{q}_\parallel J_n^2(\xi)\Lambda_2(\mathbf{q}, \omega_0 + \Omega_\mathbf{q} - n\omega) \tag{10}$$

is the time-averaged damping force, S_p is the time-averaged rate of the electron energy-gain from the HF field, $\frac{1}{2}N_e e(\mathbf{E}_\mathrm{s}\cdot\mathbf{v}_2 + \mathbf{E}_\mathrm{c}\cdot\mathbf{v}_1)$, which can be written in a form obtained from the right-hand side of equation (10) by replacing the $\mathbf{q}_\parallel$ factor with $n\omega$, and W is the time-averaged rate of the electron energy-loss due to coupling with phonons, whose expression can be obtained from the second term on the right hand side of equation (10) by replacing the $\mathbf{q}_\parallel$ factor with $\Omega_\mathbf{q}$, the energy of a wavevector-$\mathbf{q}$ phonon. The oscillating frictional force amplitudes $\mathbf{F}_\mathrm{s} \equiv \mathbf{F}_{22} - \mathbf{F}_{11}$ and $\mathbf{F}_\mathrm{c} \equiv \mathbf{F}_{21} + \mathbf{F}_{12}$ are given by ($\mu = 1, 2$)

$$\mathbf{F}_{1\mu} = -\sum_{\mathbf{q}_\parallel} \mathbf{q}_\parallel \eta_\mu |U(\mathbf{q}_\parallel)|^2 \sum_{n=-\infty}^{\infty} \left[J_n^2(\xi)\right]' \Pi_1(\mathbf{q}_\parallel, \omega_0 - n\omega) - \sum_{\mathbf{q}} \mathbf{q}_\parallel \eta_\mu |M(\mathbf{q})|^2 \sum_{n=-\infty}^{\infty} \left[J_n^2(\xi)\right]' \Lambda_1(\mathbf{q}, \omega_0 + \Omega_\mathbf{q} - n\omega), \tag{11}$$

$$\mathbf{F}_{2\mu} = \sum_{\mathbf{q}_\parallel} \mathbf{q}_\parallel \frac{\eta_\mu}{\xi} |U(\mathbf{q}_\parallel)|^2 \sum_{n=-\infty}^{\infty} 2n J_n^2(\xi)\Pi_2(\mathbf{q}_\parallel, \omega_0 - n\omega) + \sum_{\mathbf{q}} \mathbf{q}_\parallel \frac{\eta_\mu}{\xi} |M(\mathbf{q})|^2 \sum_{n=-\infty}^{\infty} 2n J_n^2(\xi)\Lambda_2(\mathbf{q}, \omega_0 + \Omega_\mathbf{q} - n\omega). \tag{12}$$

In these expressions, $\eta_\mu \equiv \mathbf{q}_\parallel \cdot \mathbf{v}_\mu/\omega\xi$, $\omega_0 \equiv \mathbf{q}_\parallel \cdot \mathbf{v}_0$, $U(\mathbf{q}_\parallel)$ and $M(\mathbf{q})$ stand for effective impurity and phonon scattering potentials, $\Pi_2(\mathbf{q}_\parallel, \Omega)$ and $\Lambda_2(\mathbf{q}, \Omega) = 2\Pi_2(\mathbf{q}_\parallel, \Omega)[n(\Omega_\mathbf{q}/T) - n(\Omega/T_\mathrm{e})]$ (with $n(x) \equiv 1/(\mathrm{e}^x - 1)$) are the imaginary parts of the electron density correlation function and electron–phonon correlation function in the presence of the magnetic field. $\Pi_1(\mathbf{q}_\parallel, \Omega)$ and $\Lambda_1(\mathbf{q}, \Omega)$ are the real parts of these two correlation functions.

The HF field enters through the argument ξ of the Bessel functions in $\mathbf{F}_0$, $\mathbf{F}_{\mu\nu}$, W and S_p. Compared with that without the HF field ($n = 0$ term only) [34], we see that in an electron gas having impurity and/or phonon scattering (otherwise homogeneous), a HF field of frequency ω opens additional channels for electron transition: an electron in a state can absorb or emit one or several photons and be scattered to a different state with the help of impurities and/or phonons. The sum over $|n| \geqslant 1$ represents contributions of single and multiple photon processes of frequency-ω photons. These photon-assisted scatterings help to transfer energy from the HF field to the electron system (S_p) and give rise to an additional damping force on the moving electrons.

Equations (6)–(9) form a closed set of equations for the determination of parameters $\mathbf{v}_0$, $\mathbf{v}_1$, $\mathbf{v}_2$ and T_e when $\mathbf{E}_0$, $\mathbf{E}_\mathrm{c}$ and $\mathbf{E}_\mathrm{s}$ are given in a 2D system subjected to a magnetic field B at temperature T. Thus they provide a comprehensive and quantitative description of transport and optical properties of magnetically biased quasi-2D semiconductors subjected to a dc bias and a HF radiation field in Faraday geometry.

Note that $\mathbf{v}_1$ and $\mathbf{v}_2$ always exhibit cyclotron resonance in the range $\omega \sim \omega_\mathrm{c}$, as can be seen from equations (7) and (8) rewritten in the form

$$\mathbf{v}_1 = \frac{\omega^2}{(\omega^2 - \omega_\mathrm{c}^2)}\left\{\frac{e}{m\omega}\left[\mathbf{E}_\mathrm{s} + \frac{e}{m\omega}(\mathbf{E}_\mathrm{c}\times\mathbf{B})\right] + \frac{1}{N_e m\omega}\left[\mathbf{F}_\mathrm{s} + \frac{e}{m\omega}(\mathbf{F}_\mathrm{c}\times\mathbf{B})\right]\right\}, \tag{13}$$

$$\mathbf{v}_2 = \frac{\omega^2}{(\omega_c^2 - \omega^2)}\left\{\frac{e}{m\omega}\left[\mathbf{E}_c - \frac{e}{m\omega}(\mathbf{E}_s \times \mathbf{B})\right] + \frac{1}{N_e m\omega}\left[\mathbf{F}_c - \frac{e}{m\omega}(\mathbf{F}_s \times \mathbf{B})\right]\right\}. \tag{14}$$

Therefore, the argument ξ may be significantly different from that of the corresponding Bessel functions in the case without a magnetic field or with a magnetic field in Voigt configuration, where the electron motion is not affected by the magnetic field [34]. On the other hand, impurity and phonon scatterings can affect ξ through the damping forces $\mathbf{F}_s$ and $\mathbf{F}_c$. Equations (13) and (14), when neglecting the damping forces $\mathbf{F}_s = 0 = \mathbf{F}_c$, yield a Bessel-function argument ξ equivalent to that used in the early literature [35, 36]. The approximation of neglecting damping forces is valid only in the weak scattering limit and away from cyclotroresonance. Depending on $\mathbf{v}_1$ and $\mathbf{v}_2$, the damping forces $\mathbf{F}_s$ and $\mathbf{F}_c$ in equations (13) and (14) are important not only in the general scattering case over the whole magnetic-field range but also in the weak scattering case in the vicinity of cyclotron resonance in that they remove the divergence and yield finite oscillation velocities $\mathbf{v}_1$ and $\mathbf{v}_2$ at $\omega = \omega_c$.

2.2. Longitudinal and transverse resistivities

The nonlinear longitudinal and transverse resistivities in the presence of a high-frequency field are easily obtained from equation (6) by choosing $\mathbf{v}_0$, i.e. the dc current, to be in the x direction, $\mathbf{v}_0 = (v_{0x}, 0, 0)$. In this paper we consider the case of a linearly polarized HF field $\mathbf{E}_t = \mathbf{E}_s \sin(\omega t)$ with $\mathbf{E}_s = (E_s, 0, 0)$ parallel to the dc current direction. Then the damping force $\mathbf{F}_0$, as given by equation (10), is also along the x direction, $\mathbf{F}_0 = (F_0, 0, 0)$, and equation (6) immediately yields

$$R_{xx} \equiv \frac{E_{0x}}{N_e e v_{0x}} = -\frac{F_0}{N_e^2 e^2 v_{0x}}, \tag{15}$$

$$R_{yx} \equiv \frac{E_{0y}}{N_e e v_{0x}} = \frac{B}{N_e e}. \tag{16}$$

The linear longitudinal resistivity is the weak dc current limit ($v_{0x} \to 0$) of (15):

$$R_{xx} = -\sum_{\mathbf{q}_\parallel} q_x^2 \frac{|U(\mathbf{q}_\parallel)|^2}{N_e^2 e^2} \sum_{n=-\infty}^{\infty} J_n^2(\xi) \frac{\partial \Pi_2}{\partial\, \Omega}\bigg|_{\Omega = n\omega} - \sum_{\mathbf{q}} q_x^2 \frac{|M(\mathbf{q})|^2}{N_e^2 e^2} \sum_{n=-\infty}^{\infty} J_n^2(\xi) \frac{\partial \Lambda_2}{\partial\, \Omega}\bigg|_{\Omega = \Omega_{\mathbf{q}} + n\omega}. \tag{17}$$

We see that the longitudinal resistivity R_{xx} is strongly affected by the irradiation through photon-assisted impurity and phonon scatterings. On the other hand, the transverse resistivity R_{xy} remains the classical form, without change in the presence of HF radiation as long as the HF and the dc currents are in the same direction. When the polarization of the HF electric field deviates from the dc current direction, however, R_{xy} can also be affected by the radiation.

Note that although according to equations (10), (15) and (17), the linear and nonlinear longitudinal magnetoresistivity R_{xx} can be formally written as the sum of contributions from various individual scattering mechanisms, all the scattering mechanisms have to be taken into account simultaneously in solving the momentum- and energy-balance equations (7)–(9) for $\mathbf{v}_1$, $\mathbf{v}_2$ and T_e, which enter the Bessel functions and other parts in the expression of R_{xx}.

2.3. Landau-level broadening

In the present model the effects of interparticle Coulomb interactions are included in the electron complex density correlation function $\Pi(\mathbf{q}_\parallel, \Omega) = \Pi_1(\mathbf{q}_\parallel, \Omega) + i\Pi_2(\mathbf{q}_\parallel, \Omega)$, which, in the random phase approximation, can be expressed as

$$\Pi(\mathbf{q}_\parallel, \Omega) = \frac{\Pi_0(\mathbf{q}_\parallel, \Omega)}{\epsilon(\mathbf{q}_\parallel, \Omega)}, \tag{18}$$

where

$$\epsilon(\mathbf{q}_\parallel, \Omega) \equiv 1 - V(q_\parallel)\Pi_0(\mathbf{q}_\parallel, \Omega) \tag{19}$$

is the complex dynamical dielectric function,

$$V(q_\parallel) = \frac{e^2}{2\epsilon_0 \kappa q_\parallel} H(q_\parallel) \tag{20}$$

is the effective Coulomb potential with κ the dielectric constant of the material and $H(q_\parallel)$ a 2D wavefunction-related overlapping integration [32], $\Pi_0(\mathbf{q}_\parallel, \Omega) = \Pi_{01}(\mathbf{q}_\parallel, \Omega) + \mathrm{i}\Pi_{02}(\mathbf{q}_\parallel, \Omega)$ is the complex density correlation function of the independent electron system in the presence of the magnetic field. With this dynamically screened density correlation function the collective plasma modes of the 2DESs are incorporated. Disregarding these collective modes one can just use a static screening $\epsilon(\mathbf{q}_\parallel, 0)$ instead.

The $\Pi_{02}(\mathbf{q}_\parallel, \Omega)$ function of a 2D system in a magnetic field can be written in terms of the Landau representation [33]:

$$\Pi_{02}(\mathbf{q}_\parallel, \Omega) = \frac{1}{2\pi l_{\mathrm{B}}^2} \sum_{n,n'} C_{n,n'}(l_{\mathrm{B}}^2 q_\parallel^2/2)\Pi_2(n, n', \Omega), \tag{21}$$

$$\Pi_2(n, n', \Omega) = -\frac{2}{\pi} \int \mathrm{d}\varepsilon\, [f(\varepsilon) - f(\varepsilon + \Omega)]\, \mathrm{Im}\, G_n(\varepsilon + \Omega)\, \mathrm{Im}\, G_{n'}(\varepsilon), \tag{22}$$

where $l_{\mathrm{B}} = \sqrt{1/|eB|}$ is the magnetic length,

$$C_{n,n+l}(Y) \equiv n![(n+l)!]^{-1} Y^l \mathrm{e}^{-Y} [L_n^l(Y)]^2 \tag{23}$$

with $L_n^l(Y)$ the associate Laguerre polynomial, $f(\varepsilon) = \{\exp[(\varepsilon - \mu)/T_{\mathrm{e}}] + 1\}^{-1}$ the Fermi distribution function and $\mathrm{Im}\, G_n(\varepsilon)$ is the imaginary part of the electron Green function, or the DOS, of the Landau level n. The real part function $\Pi_{01}(\mathbf{q}_\parallel, \Omega)$ and corresponding $\Lambda_{01}(\mathbf{q}_\parallel, \Omega)$ function can be derived from their imaginary parts via the Kramers–Kronig relation.

In principle, to obtain the Green function $\mathrm{Im}\, G_n(\varepsilon)$, a self-consistent calculation has to be carried out from the Dyson equation for the self-energy with all the impurity, phonon and other scatterings included. The resultant G_n is generally a complicated function of the magnetic field, temperature and Landau-level index n, also dependent on the relative strengths of different kinds of scatterings [37, 38]. In the present study we do not attempt a self-consistent calculation of $G_n(\varepsilon)$. Instead, we choose a Gaussian-type form [37] for the purpose of demonstrating the observed oscillations (ε_n is the energy of the nth Landau level):

$$\mathrm{Im}\, G_n(\varepsilon) = -\sqrt{\frac{\pi}{2\Gamma^2}} \exp\left[-\frac{(\varepsilon - \varepsilon_n)^2}{2\Gamma^2}\right] \tag{24}$$

with a broadening width given by

$$\Gamma = \left(\frac{2e\omega_{\mathrm{c}}\alpha}{\pi m \mu_0(T)}\right)^{1/2}, \tag{25}$$

where $\mu_0(T)$ is the linear mobility at temperature T in the absence of the magnetic field and $\alpha > 1$ is a semiempirical parameter to take account of the difference in the transport scattering time determining the mobility $\mu_0(T)$, to which larger angle scattering contributes a heavier weight, from the single particle lifetime, to which scattering with small or large angle equally contributes [4, 12, 14].

3. GaAs-based 2DESs

Similar to recent experiments, we focus our attention on two ultra high mobility two-dimensional electron systems of GaAs/AlGaAs heterostructure with same electron sheet density $N_e = 3 \times 10^{11}$ cm^{-2} but having linear mobility $\mu_0(1\ \mathrm{K}) = 2.4 \times 10^7$ cm^2 V^{-1} s^{-1} and $\mu_0(1\,\mathrm{K}) = 1.46 \times 10^7$ cm^2 V^{-1} s^{-1}, respectively, in the absence of magnetic field. In GaAs/AlGaAs systems, phonon modes and electron–phonon couplings are well established [32]. We consider both transverse acoustic phonons (interacting with electrons via piezoelectric coupling) and longitudinal acoustic phonons (interacting with electrons via piezoelectric and deformation potential couplings). We assumed that the elastic scatterings are due to the remote charged impurities which are located a distance $s = 60$ nm away from the interface of the heterojunction in the barrier side. The impurity densities are determined by the requirement that the electron total linear mobility equals the given value at temperature $T = 1$ K. The effective impurity scattering potentials $|U(\mathbf{q}_\parallel)|^2$ and electron–phonon matrix elements $|M(\mathbf{q})|^2$ as discussed earlier in [32] are used in the calculation, with full inelasticity of electron couplings with both longitudinal and transverse phonons included. The material and coupling parameters for the system are well defined and taken as: electron effective mass $m = 0.068\, m_e$ (m_e is the free electron mass), transverse sound speed $v_{st} = 2.48 \times 10^3$ m s^{-1}, longitudinal sound speed $v_{sl} = 5.29 \times 10^3$ m s^{-1}, acoustic deformation potential $\Xi = 8.5$ eV, piezoelectric constant $e_{14} = 1.41 \times 10^9$ V m^{-1}, dielectric constant $\kappa = 12.9$, material mass density $d = 5.31$ g cm^{-3}. The depletion layer charge number density is taken as $N_{dep} = 5 \times 10^{10}$ cm^{-2}.

In GaAs system at low temperatures $\mu_0(T)$ comes from impurity, transverse and longitudinal acoustic phonon scatterings:

$$\frac{1}{\mu_0} = \frac{1}{\mu_0^{(i)}} + \frac{1}{\mu_0^{(pt)}} + \frac{1}{\mu_0^{(pl)}}. \tag{26}$$

The longitudinal magnetoresistivity R_{xx} (equation (17)) consists of contributions from the impurity, transverse and longitudinal acoustic phonon scatterings. In the following sections we will carry out numerical calculations for R_{xx} assuming linearly polarized MW fields ($\mathbf{E}_c = 0$) with multiphoton processes included.

The microwave field intensity required for the appearance of resistivity oscillation in these high-mobility samples is moderate. The slight electron heating induced by the irradiation in these systems is unimportant as far as the main phenomenon is concerned. As can be seen later, the radiation-induced magnetoresistance oscillation is not sensitive to the moderate rise of electron temperature. Therefore, R_{xx} can be obtained directly from equation (17) with $T_e = T$. We will check the effect of the elevated electron temperature in section 4.1.3.

4. R_{xx} at temperature $T = 1$ K

4.1. Impurity-induced magnetoresistivity

4.1.1. Linear resistivity. We assume that the elastic scatterings are due to ionized remote impurities [32]. Figure 1(a) shows the impurity-induced longitudinal resistivity R_{xx} versus $\omega/\omega_c \equiv \gamma_c$ subjected to a microwave radiation of frequency $\omega/2\pi = 0.1$ THz at four values of amplitude: $E_s = 15$, 30, 45 and 60 V cm^{-1}, together with dark resistivity curve ($E_s = 0$). At temperature $T = 1$ K Shubnikov–de Haas (SdH) oscillations of period $\gamma_c = 0.039$ show up strongly on the high ω_c side, and then gradually decay away as $1/\omega_c$ increases. In addition to this, all four resistivity curves exhibit clear oscillation having the main oscillation period $\gamma_c = 1$

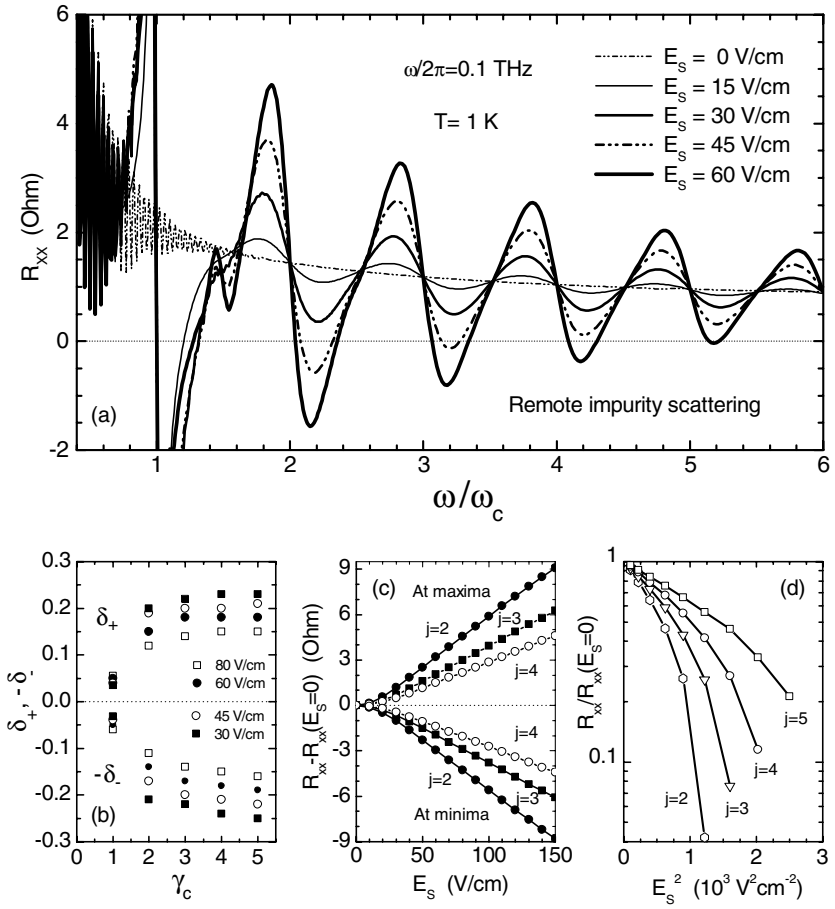

Figure 1. (a) The longitudinal linear magnetoresistivity R_{xx} induced by remote-impurity scattering in a GaAs-based heterosystem subjected to crossed magnetic fields B and in-plane linearly polarized HF fields $E_s \sin(\omega t)$ of frequency $\omega/2\pi = 0.1$ THz with several different amplitudes at lattice temperature $T = 1$ K. $\omega_c \equiv eB/m$ stands for the cyclotron frequency. The other parameters are: electron density $N_e = 3.0 \times 10^{11}$ cm^{-2}, zero-magnetic-field linear dc mobility $\mu_0(1\,\mathrm{K}) = 2.4 \times 10^7$ cm^2 V^{-1} s^{-1}, and the broadening coefficient $\alpha = 12$. The electron temperature is set to be $T_e = T$. (b) Parameters δ_+ and δ_- for locations of resistance maxima and minima at several HF field amplitudes. (c) The photoresistivity $R_{xx} - R_{xx}(E_s = 0)$ at maxima and at minima of $j = 1$ and 2 against the amplitude of the HF field. (d) $R_{xx}/R_{xx}(E_s = 0)$ is shown against E_s^2 on logarithmic scale for $j = 2$, 3 and 4.

(they cross at integer points $\gamma_c = 2, 3, 4, 5$). The resistivity maxima locate around $\gamma_c = j - \delta_-$ and minima around $\gamma_c = j + \delta_+$ with $\delta_\pm \sim 0.14$–0.26 for $j = 3, 4, 5$, $\delta_\pm \sim 0.11$–0.22 for $j = 2$, and $\delta_\pm \sim 0.03$–0.07 for $j = 1$ (figure 1(b)). The amplitude of the oscillation increases with increasing HF field intensity for $\gamma_c > 1.5$. Resistivity becomes negative for $E_s = 60$ V cm^{-1} around the minima at $j = 1, 2, 3, 4$ and 5, for $E_s = 45$ V cm^{-1} at $j = 1, 2$ and 3, and for $E_s = 30$ and 15 V cm^{-1} at $j = 1$. These main peak-valley structures are related to single-photon ($|n| = 1$) processes. In the vicinity of $\gamma_c = 1$, where the cyclotron resonance greatly enhances the effective amplitude of the HF field in photon-assisted scatterings, multiphoton processes show up. The amplitudes of the $j = 1$ maximum and minimum no longer monotonically change with field intensity. Furthermore, there appears

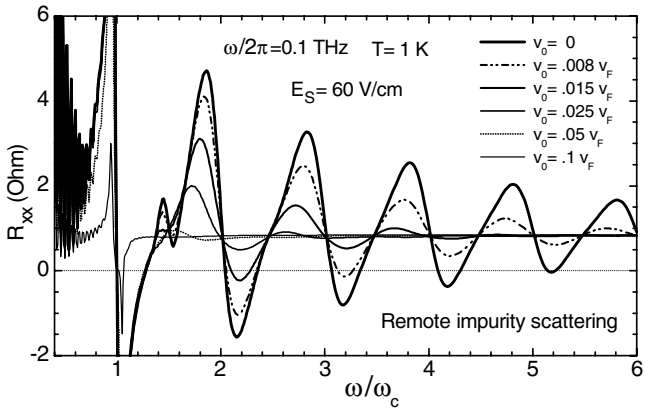

Figure 2. Remote-impurity induced nonlinear longitudinal magnetoresistivity R_{xx} as defined in equation (15) in the GaAs-based 2DEG subjected to crossed magnetic fields B and an in-plane linearly polarized HF field $E_s \sin(\omega t)$ of frequency $\omega/2\pi = 0.1$ THz and amplitude $E_s = 60$ V cm^{-1} under several different dc bias velocities $v_0 = 0, 0.008, 0.015, 0.025, 0.05$ and $0.1v_F$, where $v_F = 2.4 \times 10^5$ m s^{-1} is the electron Fermi velocity. $\omega_c \equiv eB/m$ is the cyclotron frequency. The other parameters are the same as indicated in figure 1.

a shoulder around $\gamma_c = 1.5$ on the curves of $E_s = 15$ and 30 V cm^{-1}, and it develops into a secondary peak in the cases of $E_s = 45$ and 60 V cm^{-1}. This peak-valley structure around $\gamma_c = 1.5$ is related to two-photon ($|n| = 2$) processes. The oscillatory peak-valley structure related to three-photon processes was demonstrated in the cases of lower microwave frequency ($\omega = 60$ and 40 GHz) [24].

The dependence of the resistivity at maxima and minima on the microwave intensity is shown in figure 1(c), where we plot the calculated photoresistivity, i.e. the magnetoresistivity in the presence of radiation, R_{xx}, minus the dark resistivity $R_{xx}(E_s = 0)$, as a function of radiation field amplitude E_s at peaks and valleys of $j = 2, 3$ and 4. We see that $|R_{xx} - R_{xx}(E_s = 0)|$ grows like E_s^2 at lower intensity and become linearly dependent on E_s at higher intensity within the amplitude range shown. This is in agreement with experiments [4–6].

Figure 1(d) shows the positive parts of $R_{xx}/R_{xx}(E_s = 0)$ at minima of $j = 2, 3$ and 4 on a logarithmic scale as functions of E_s^2.

4.1.2. Nonlinear resistivity. Figure 2 shows the nonlinear longitudinal resistivity R_{xx} due to remote-impurity scattering calculated directly from equation (15) for the 2DESs subject to a 0.1 THz microwave radiation of amplitude $E_s = 60$ V cm^{-1} under different dc bias velocities $v_0 = 0, 0.008, 0.015, 0.025, 0.05$ and $0.1\ v_F$, where the electron Fermi velocity $v_F = 2.4 \times 10^5$ m s^{-1}. For the given strength of the radiation field the linear magnetoresistivity (vanishing E_0 or v_0) exhibits the strongest oscillation. A finite dc bias always suppresses the oscillation and may destroy the negative resistivity appearing at vanishing dc bias. The effect is apparently much stronger at larger γ_c than at smaller γ_c.

4.1.3. Effect of elevated electron temperature. Upon microwave irradiation the electron temperature can be higher than the lattice temperature. To have an idea of how the elevated electron temperature affects the magnetoresistivity oscillation we show in figure 3 the remote-impurity induced longitudinal resistivity R_{xx} of the 2DEG having electron temperatures $T_e = 1, 5$ or 50 K but at the same lattice temperature $T = 1$ K subject to a microwave

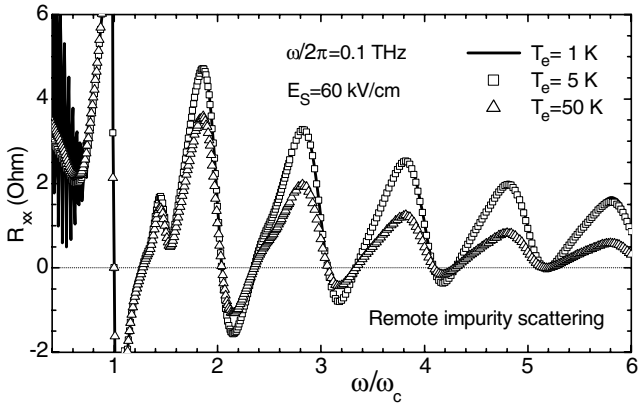

Figure 3. The impurity-induced linear magnetoresistivity R_{xx} of a GaAs-based 2DES subjected to a microwave field of amplitude $E_s = 60$ V cm^{-1} and frequency $\omega/2\pi = 0.1$ THz at elevated electron temperatures. The lattice temperature is $T = 1$ K. The other parameters are the same as indicated in figure 1.

irradiation of frequency $\omega/2\pi = 0.1$ THz and amplitude $E_s = 60$ kV cm^{-1}. We see that at $T_e = 5$ K SdH oscillations disappear completely, but the radiation-induced oscillations remain essentially the same. Only when the electron temperature becomes much higher, e.g. 50 K, can the appreciable change in the resistance oscillation curve be observed. This indicates that the radiation-induced resistivity oscillation is quite insensitive to electron temperature and we can analyse the moderate-strength microwave induced resistivity oscillation by neglecting the electron temperature change in the system. On the other hand, using a slightly elevated electron temperature provides a way to separate the radiation-induced oscillation from the SdH effect.

Experiments indicated that the strongest SdH oscillations always show up on the dark resistivity curve and with enhancing the radiation intensity the SdH oscillations weaken [4, 6]. This fact can be easily understood to be due to the rise of the electron temperature caused by the microwave illumination: SdH oscillations are suppressed by the rising electron temperature, while the radiation-induced R_{xx} oscillations remain the same as long as the lattice temperature remains unchanged.

4.2. Acoustic-phonon-induced magnetoresistivity

Acoustic phonon scattering has recently been proposed as a mechanism of the absolute negative resistivity leading to the vanishing resistance state [26, 27]. To check such a possibility we show in figure 4 the linear magnetoresistivity R_{xx}, contributed separately by transverse acoustic phonon scattering (a) and by longitudinal acoustic phonon scattering (b), as functions of ω/ω_c under 0.1 THz microwave illumination of different strengths. Photon-assisted acoustic-phonon scattering itself indeed can give rise to a pronounced resistance oscillation with changing magnetic field and R_{xx} at oscillation minima can go down to negative under microwave irradiations for both transverse and longitudinal phonon scatterings. These acoustic-phonon induced R_{xx} oscillations, however, exhibit quite different behaviour from that of the impurity-induced R_{xx} oscillations shown in figure 1 and are also different from each other.

Note that, at temperature $T = 1$ K, the acoustic phonon scattering produces a part of R_{xx} which is more than an order of magnitude smaller than that contributed from impurity scattering in the system having a mobility of 2.4×10^7 cm^2 V^{-1} s^{-1} at $T = 1$ K. Therefore, acoustic

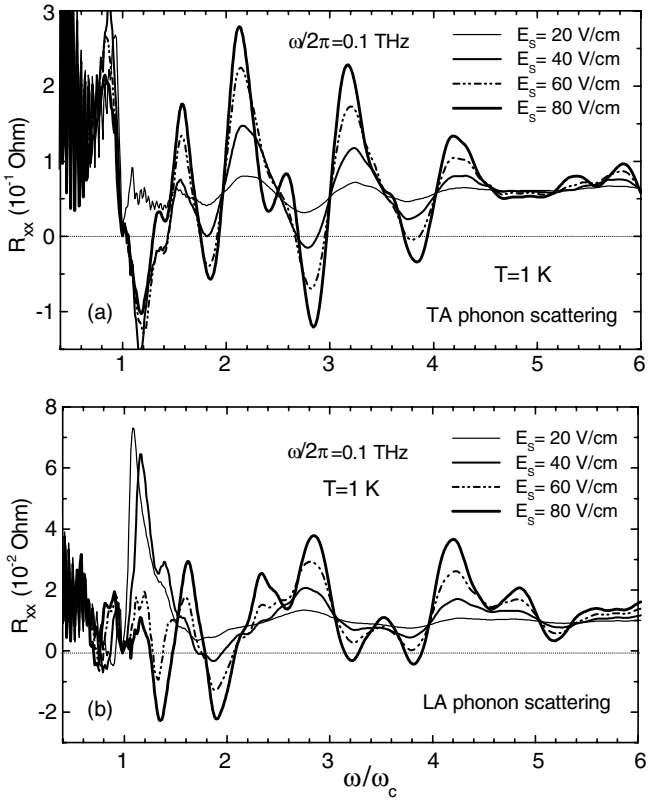

Figure 4. Linear magnetoresistivities R_{xx} induced by transverse acoustic phonons (a) and by longitudinal acoustic phonons (b) in a GaAs-based 2DES subjected to microwave fields $E_s \sin(\omega t)$ of frequency $\omega/2\pi = 0.1$ THz having different amplitudes. The lattice temperature is $T = 1$ K and the electron temperature $T_e = T$. The other parameters are: electron density $N_e = 3.0\times10^{11}$ cm^{-2}, dc mobility $\mu_0(1\,\mathrm{K}) = 2.4 \times 10^7$ cm^2 V^{-1} s^{-1} and broadening coefficient $\alpha = 12$.

phonon scattering essentially gives no direct contribution to the experimentally observed resistance oscillation at this low temperature. Nevertheless, acoustic phonons play a key role in suppressing the resistance oscillation at elevated lattice temperatures. We will discuss this issue in section 5.

5. Effect of elevated lattice temperature

One of the most important aspects of the experimental finding on the magnetoresistance oscillation in irradiated 2DESs is the temperature dependence of R_{xx}. Experiments [4, 5] found that the 'zero-resistance' states and radiation-induced magnetoresistance oscillations show up strongly only at low temperatures typically around $T = 1$ K or lower. At fixed microwave power with increasing temperature, not only the zero-resistance regions become narrower and eventually disappear, the whole oscillatory structure (peaks and valleys) diminishes as well. At temperature $T \geqslant 4$–5 K, the oscillatory structure disappears completely and the resistivity R_{xx} versus magnetic field becomes essentially flat [5].

Both groups analysed the temperature variation of R_{xx} at deepest minima using an activated-type dependence $\exp(-T_0/T)$. The activation energies observed by them are very

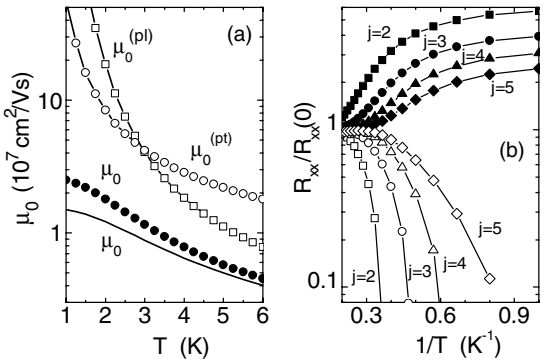

Figure 5. (a) Zero-magnetic-field linear mobility induced by transverse acoustic phonon scattering, $\mu_0^{(pt)}$, by longitudinal acoustic phonon scattering, $\mu_0^{(pl)}$, and total mobility μ_0, for the system with $\mu_0(1\ \mathrm{K}) = 2.4 \times 10^7\ \mathrm{cm^2\ V^{-1}\ s^{-1}}$ (dots), and for the system with $\mu_0(1\ \mathrm{K}) = 1.46 \times 10^7\ \mathrm{cm^2\ V^{-1}\ s^{-1}}$ (solid curve). (b) The ratios of $R_{xx}(T)/R_{xx}(0)$ at maxima and at minima are shown against $1/T$ on a logarithmic scale for $j = 2, 3, 4$ and 5. The system is that described in figure 6 and $R_{xx}(0)$ is the resistivity at $T = 1$ K in the absence of magnetic field.

high and different: up to 10 and 20 K at $j = 1$ minimum [4, 5]. The different T_0 values observed by the two groups indicate that the speed of the oscillatory structure disappearing with temperature is sample dependent [4, 5]. To explain the temperature dependence the formation of an energy gap around the Fermi surface in the spectrum is suggested under microwave irradiation around the resistance minima [4].

Our explanation of the temperature dependence of the magnetoresistance oscillations is based on the temperature variation of the Landau level broadening Γ as determined by equation (25). In a GaAs-based system, when the lattice temperature increases from around $T = 1$ K, the numbers of transverse and longitudinal acoustic phonons and thus the electron–phonon scattering strengths increase rapidly. In figure 5(a) we plot the zero-magnetic-field linear mobility $\mu_0^{(pt)}$ due to transverse acoustic phonon scattering, $\mu_0^{(pl)}$ due to longitudinal phonon scattering, and the total mobility μ_0 (dots) as functions of lattice temperature T for the GaAs-based heterosystem with $\mu_0 = 2.4 \times 10^7\ \mathrm{cm^2\ V^{-1}\ s^{-1}}$ at $T = 1$ K. We see that when temperature T rises from 1 to 3 K the phonon related mobilities decline by about an order of magnitude, leading to the total mobility $\mu_0(T)$ decreasing by about a factor of 2.2 and, according to (25), Γ increasing by about a factor of 1.5 (assuming α unchanged). The temperature growth of the Landau-level width due to this enhanced phonon scattering results in the strong temperature variation of the radiation-induced magnetoresistance oscillation. Figure 6 shows the calculated linear resistivity R_{xx} due to remote-impurity scattering as a function of ω/ω_c at different lattice temperatures $T = 1.0, 1.5, 2.0, 2.5, 3.0, 3.5, 4.0$ and 5.0 K for the system of $\mu_0(1\ \mathrm{K}) = 2.4 \times 10^7\ \mathrm{cm^2\ V^{-1}\ s^{-1}}$ under a fixed microwave illumination of frequency $\omega/2\pi = 0.1$ THz and amplitude $E_s = 60\ \mathrm{V\ cm^{-1}}$. The broadening parameter is fixed to be $\alpha = 12$ for all the curves of different lattice temperatures, and the electron temperature is taken to be equal to the lattice temperature in all the calculations in this section. The sensitive temperature dependence of the resistance oscillation is quite obvious. The magnitude of peaks and valleys of the oscillation diminishes straightforwardly with increasing temperature from 1 K. At $T \geqslant 5$ K the oscillation structure almost disappears and R_{xx} exhibits quite a flat form with changing ω/ω_c for $\gamma_c \geqslant 1.1$.

To show the temperature variation of R_{xx}, we plot in figure 5(b) the values of R_{xx} at peaks and the positive values at valleys (divided by $R_{xx}(0)$, the resistivity at $T = 1$ K in the absence

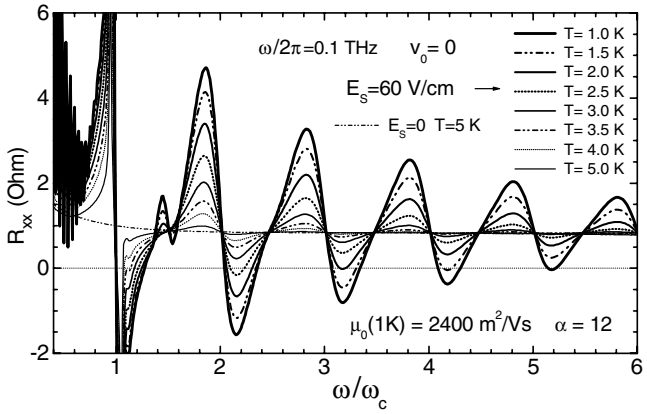

Figure 6. The longitudinal magnetoresistivity R_{xx} induced by remote impurity scattering at different lattice temperatures $T = 1.0, 1.5, 2.0, 2.5, 3.0, 3.5, 4.0$ and 5.0 K for a GaAs-based 2DEG subjected to a HF field $E_s \sin(\omega t)$ of frequency $\omega/2\pi = 0.1$ THz and amplitude $E_s = 80$ V cm^{-1}. The system parameters are: electron density $N_e = 3.0 \times 10^{11}$ cm^{-2}, dc mobility $\mu_0 = 2.4 \times 10^7$ cm^2 V^{-1} s^{-1} at $T = 1$ K, and the broadening coefficient $\alpha = 12$ for all the curves. Also shown is the dark resistivity ($E_s = 0$) at $T = 5$ K.

of the magnetic field) against $1/T$ on a logarithmic scale. If we roughly fit the data with the form $R_{xx}(T) \propto \exp(-T_0/T)$, we have $T_0 \approx 13$ K for $j = 2$, $T_0 \approx 9.5$ K for $j = 3$, $T_0 \approx 5$ K for $j = 4$ and $T_0 \approx 3.3$ K for $j = 5$ on average over the range shown.

The sensitivity of the temperature variation of the radiation-induced magnetoresistance oscillation is sample dependent. In GaAs-based systems the electron–phonon scattering strengths, thus the acoustic-phonon induced mobilities $\mu_0^{(\mathrm{pt})}$ and $\mu_0^{(\mathrm{pl})}$, and their temperature behaviour are essentially the same. Therefore, the temperature variation of the total mobility μ_0 depends mainly on the strength of the impurity scattering, which is almost temperature independent within this range of T. The lowest curve in figure 5(a) shows the T-dependence of the total mobility $\mu_0(T)$ for the sample having $T = 1$ K mobility $\mu_0(1\ \mathrm{K}) = 1.46 \times 10^7$ cm^2 V^{-1} s^{-1}, which apparently exhibits a slower temperature change than that of the $\mu_0(1\ \mathrm{K}) = 2.4 \times 10^7$ cm^2 V^{-1} s^{-1} system.

In figure 7 we illustrate the linear resistivity R_{xx} induced by remote impurity scattering as a function of ω/ω_c at different lattice temperatures $T = 1.0, 1.5, 2.0, 2.5, 3.0, 3.5, 4.0, 5.0$ and 6.0 K for the system of $\mu_0(1\ \mathrm{K}) = 1.46 \times 10^7$ cm^2 V^{-1} s^{-1} under a fixed microwave irradiation of frequency $\omega/2\pi = 0.1$ THz and amplitude $E_s = 45$ V cm^{-1}. The broadening parameter is fixed to be $\alpha = 7.3$ for all the lattice temperatures. The speed of the oscillatory structure disappearing with rising temperature is apparently slower than the system shown in figure 6.

6. Conclusion

Based on the balance-equation model for magnetotransport in Faraday geometry, we have carried out a detailed theoretical investigation on microwave-radiation induced magnetoresistance oscillations recently discovered in high-mobility GaAs-based two-dimensional electron systems. We find that for systems having zero-field linear mobility $\mu_0(1\ \mathrm{K}) \leqslant 2.4 \times 10^7$ cm^2 V^{-1} s^{-1}, multiphoton-assisted impurity scatterings are the main mechanisms responsible for radiation-induced magnetoresistance oscillations at temperature

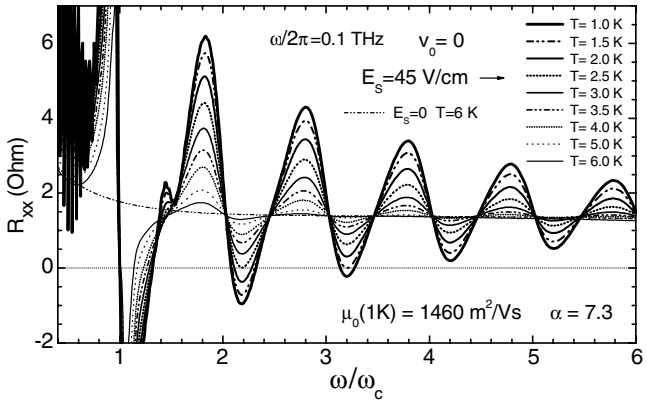

Figure 7. The longitudinal magnetoresistivity R_{xx} induced by remote impurity scattering at different lattice temperature $T = 1.0, 1.5, 2.0, 2.5, 3.0, 3.5, 4.0, 5.0$ and 6.0 K for a GaAs-based 2DEG subjected to a HF field $E_s \sin(\omega t)$ of frequency $\omega/2\pi = 0.1$ THz and amplitude $E_s = 45$ V cm^{-1}. The system parameters are: electron density $N_e = 3.0 \times 10^{11}$ cm^{-2}, dc mobility $\mu_0(1\text{ K}) = 1.46 \times 10^7$ cm^2 V^{-1} s^{-1}, broadening coefficient $\alpha = 7.3$ for all the curves. Also shown is the dark resistivity ($E_s = 0$) at $T = 6$ K.

$T \leqslant 4$ K. The amplitude of the R_{xx} oscillation grows roughly following the microwave power under weak illumination, and following the microwave amplitude under medium illumination, before it saturates and even decreases with a continuing increase of the microwave strength under strong irradiation. It is shown that the strongest oscillations appear in the linear longitudinal magnetoresistance and a finite dc current bias always suppresses the oscillation. Different from the SdH oscillation which is easily suppressed by a few-degree rise of the electron temperature, the radiation-induced magnetoresistance oscillations are quite insensitive to the modest electron heating as long as the lattice temperature remains the same. Although the magnetoresistivities directly stemming from photon-assisted transverse and longitudinal acoustic phonon scatterings also exhibit pronounced oscillations under microwave irradiation, they contribute only a small part of the total R_{xx} in the temperature range of $T \leqslant 4$ K. Nevertheless, it is just this acoustic phonon scattering that gives rise to the sensitive lattice temperature dependence of radiation-induced resistance oscillations right from $T = 1$ K. We have shown that the growth of the Landau level broadening resulting from the enhancement of acoustic phonon scatterings with increasing lattice temperature leads to the observed temperature suppression of the oscillation.

Acknowledgments

The author is grateful to Dr S Y Liu for helpful discussions. This work was supported by Major Projects (10390161, 90103067) of the National Natural Science Foundation of China, the Special Funds for Major State Basic Research Project (G20000683) and the Shanghai Municipal Commission of Science and Technology (03DJ14003).

References

[1] Zudov M A, Du R R, Simmons J A and Reno J L 2001 *Phys. Rev.* B **64** 201311(R)
[2] Ye P D, Engel L W, Tsui D C, Simmons J A, Wendt J R, Vawter G A and Reno J L 2001 *Appl. Phys. Lett.* **79** 2193

[3] Mani R G, Smet J H, von Klitzing K, Narayanamurti V, Johnson W B and Umansky V 2003 *Proc. 26th Int. Conf. on the Physics of Semiconductors (Edinburgh, 2002)* (*Inst. Phys. Conf. Ser. 171*) ed A C Long and J H Davis H112
[4] Mani R G, Smet J H, von Klitzing K, Narayanamurti V, Johnson W B and Umansky V 2002 *Nature* **420** 646
[5] Zudov M A, Du R R, Pfeiffer L N and West K W 2003 *Phys. Rev. Lett.* **90** 046807
[6] Mani R G, Smet J H, von Klitzing K, Narayanamurti V, Johnson W B and Umansky V 2003 *Preprint* cond-mat/0306388
[7] Zudov M A 2003 *Phys. Rev.* B **69** 041304
[8] Kohn W 1961 *Phys. Rev.* **123** 1242
[9] Dorozhkin S I 2003 *JETP Lett.* **77** 577
[10] Willett R L, West K W and Pfeiffer L N 2003 *Bull. Am. Phys. Soc.* **48** 459
[11] Yang C L, Zudov M A, Knuuttila T A, Du R R, Pfeiffer L N and West K W 2003 *Phys. Rev. Lett.* **91** 096803
[12] Durst A C, Sachdev S, Read N and Girvin S M 2003 *Phys. Rev. Lett.* **91** 086803
[13] Andreev A V, Aleiner I L and Millis A J 2003 *Phys. Rev. Lett.* **91** 056803
[14] Anderson P W and Brinkman W F 2003 *Preprint* cond-mat/0302129
[15] Shi J and Xie X C 2003 *Phys. Rev. Lett.* **91** 086801
[16] Phillips J C 2003 *Preprint* cond-mat/0303181
[17] Koulakov A A and Raikh M E 2003 *Preprint* cond-mat/0302465
[18] Mikhailov S A 2003 *Preprint* cond-mat/0303130
[19] Lee D-H and Leinaas J M 2003 *Preprint* cond-mat/0305302
[20] Ryzhii V I 1970 *Sov. Phys.—Solid State* **11** 2087
[21] Ryzhii V I, Suris R A and Shchamkhalova B S 1986 *Sov. Phys.—Semicond.* **20** 1299
[22] Keay B J, Zeuner S, Allen S J, Maranowski K D, Gossard A C, Bhattacharya U and Rodwell M J W 1995 *Phys. Rev. Lett.* **75** 4102
[23] Tien P K and Gordon J P 1963 *Phys. Rev.* **129** 647
[24] Lei X L and Liu S Y 2003 *Phys. Rev. Lett.* **91** 226805
[25] Vavilov M G and Aleiner I L 2004 *Phys. Rev.* B **69** 035303
[26] Ryzhii V I and V'yurkov V V 2003 *Phys. Rev.* B **68** 165406
[27] Ryzhii V I 2003 *Phys. Rev.* B **68** 193402
[28] Ryzhii V I 2003 *Preprint* cond-mat/0305484
[29] Ryzhii V I and Suris R A 2003 *J. Phys.: Condens. Matter* **15** 6855
[30] Liu S Y and Lei X L 2003 *J. Phys.: Condens. Matter* **15** 4411
[31] Lei X L and Ting C S 1985 *Phys. Rev.* B **32** 1112
[32] Lei X L, Birman J L and Ting C S 1985 *J. Appl. Phys.* **58** 2270 and the references therein.
[33] Ting C S, Ying S C and Quinn J J 1977 *Phys. Rev.* B **14** 5394
[34] Lei X L 1998 *J. Appl. Phys.* **84** 1396
Lei X L 1998 *J. Phys.: Condens. Matter* **10** 3201
[35] Malov A D and Ryzhii V I 1973 *Sov. Phys.—Solid State* **14** 1766
[36] V'yurkov V V, Gladun A D, Malov A D and Ryzhii V I 1977 *Fiz. Tverd. Tela* **19** 3618
[37] Ando T, Fowler A B and Stern F 1982 *Rev. Mod. Phys.* **54** 437
[38] Leadley D R, Nicholas R J, Xu W, Peeters F M, Devreese J T, Singleton J, Perenboom J A A J, van Bockstal I, Herlach F, Foxon C T and Harris J J 1993 *Phys. Rev.* B **48** 5457